CrossMark

ORIGINAL PAPER

Synthesis and characterization of agarose–bacterial cellulose biodegradable composites

Ankur Awadhiya[1] · David Kumar[2] · Kalpana Rathore[3] ·
Bushara Fatma[3] · Vivek Verma[3,4]

Abstract Agarose is an abundant and biodegradable polymer with strength comparable or higher than other commonly used natural polymers. Agarose can be used for wound dressing and tissue engineering applications. Excessive water uptake and moderate strength limit its applicability for various applications. The objective of this study was to enhance its strength by reinforcing with bacterial cellulose. The addition of bacterial cellulose exhibited remarkable enhancement of 140% in the tensile strength of agarose bioplastic. The strength increased from 25.1 MPa for agarose bioplastic to a maximum of 60.2 MPa for 20% (w/w) of bacterial cellulose. There was a decrease in the amount of water absorption; at 37 °C, the composite films absorbed 450% of their own weight of water, as against 700% absorption by un-reinforced bioplastic films at the same temperature. Thermogravimetric analysis did not reveal any perceivable change in the thermal stability of the bioplastic. Biodegradability of composite films was also established.

Keywords Agarose · Bacterial cellulose · Bioplastic · Fiber-reinforced composite

✉ Vivek Verma
  vverma@iitk.ac.in

1 Department of Biological Sciences and Bioengineering, Indian Institute of Technology Kanpur, Kanpur, India

2 Department of Aerospace Engineering, Indian Institute of Technology Kanpur, Kanpur, India

3 Department of Materials Science and Engineering, Indian Institute of Technology Kanpur, Kanpur, India

4 Centre for Environmental Science and Engineering, Indian Institute of Technology Kanpur, Kanpur, India

Abbreviations

UTS   Ultimate tensile strength
HBC   Homogenized bacterial cellulose
TGA   Thermogravimetric analysis

Introduction

Bioplastics are biodegradable plastics, often made from biological resources. They have been prepared from a variety of raw materials, including starch [1], proteins [2, 3], polyesters [4] and poly(hydroxyalkanoate)s [5, 6]. While bioplastics are sustainable and eco-friendly alternatives to petroleum-based plastics, their applicability is restricted by their properties, especially low strength and high water absorption when compared to petro-plastics. These properties are often enhanced through physical methods like reinforcement [2, 7], and chemical methods such as cross-linking [8].

Agarose is a biodegradable polymer [9–11] made of D-galactose and 3,6-anhydro-L-galactopyranose. It has strength comparable or even higher than other commonly used natural polymers such as starch [1, 12, 13] that makes it suitable for developing bioplastic. The role of agarose for wound dressing [14] and tissue engineering [9, 15] applications has been explored. Agarose has moderate mechanical properties that need to be addressed before using it in packaging applications. In earlier studies, mechanical properties of agarose were improved by adding various types of fillers. Lewitus et al. used carbon nanomaterials for improving mechanical properties of agarose to develop scaffolds for tissue engineering applications [16]. Li et al. significantly increased tensile strength and modulus of agarose by adding nanoclay [17]. Le Goff et al. improved rheological mechanical properties of agarose by reinforcing it with cellulose nanowhiskers [18]. Chemical crosslinking of agarose films using citric acid demonstrated increased strength and reduced water uptake of the films [19]. Agarose-based composites had been studied for tissue engineering applications where cellulose was used as reinforcement [20]. Agarose was also investigated as a potential biomaterial [21, 22]. In this paper, we describe reinforcing of agarose bioplastic with bacterial cellulose. We refer agarose bioplastics as agarose with 20% (v/w) glycerol as plasticizer.

Cellulose is a natural polysaccharide made of $\beta(1 \rightarrow 4)$ linked D-glucose that has been used as a reinforcement agent with several polymers such as agar [23, 24], PVA [25–27], latex [28], starch [2] and epoxy [29]. Li et al. [30] studied the structure–morphology–rheology relationships of cellulose nanoparticles. They showed the effect of hydrolysis time on the rheological properties of cellulose nanofibers (CNFs) and cellulose nanocrystals (CNCs). Deng et al. [31] synthesized microcrystalline cellulose-graft-poly (methyl methacrylate) copolymer for reinforcing the rubber. In this study, we have employed bacterial cellulose (BC) to increase the mechanical strength of agarose matrix. Bacterial cellulose has become an excellent reinforcement due to its high mechanical strength and crystallinity.

Bacterial cellulose and its composites have also been used for tissue engineering applications [32–35].

Fundamental drawbacks associated with agarose are its excessive water uptake capability and low strength in comparison to commonly used synthetic polymers. The objective of this study is to increase the mechanical strength and decrease the water uptake capability of agarose without compromising its biodegradability. To achieve this, bacterial cellulose is used as a reinforcing filler for agarose. Developed agarose–bacterial cellulose composites are characterized for their mechanical and thermal properties, and biodegradability.

Materials and methods

Materials

Agarose was purchased from Merck Specialties Private Limited, Mumbai, and was used without further modifications. Glycerol and methylene blue were purchased from Qualigens Fine Chemicals, Mumbai. Disodium hydrogen phosphate, citric acid and glucose were purchased from Fisher Scientific, Mumbai, and sodium hydroxide, yeast extract and peptone powder were procured from Loba Chemie, Mumbai. The tissue homogenizer used was T18 Digital from IKA. *Acetobacter xylinum Yamada* (ATCC 53582) bacteria were received as a kind gift from Dr. Jeffrey M. Catchmark of The Pennsylvania State University.

Culture of *Acetobacter xylinum*, harvesting of bacterial cellulose and generation of homogenized bacterial cellulose (HBC)

Bacteria were cultivated in a modified Hestrin–Schramm medium [36], containing 2.0% D-glucose, 0.5% peptone, 0.5% yeast extract, 0.115% citric acid, 0.27% disodium hydrogen phosphate and 1% ethanol in water. The pH was kept at 6.0, as described earlier [37], and the medium was autoclaved at 121 °C for 20 min prior to use. A 10 mL of primary culture was set up with a picked-up colony of *A. xylinum*. After cultivation under static conditions for 4 days at 30 °C, the primary culture was added to a 1-L bottle of modified Hestrin–Schramm medium. After thorough mixing, 50 mL of the suspension was added to 100-mm Petri dishes, which were then kept at 30 °C. After further 10 days of cultivation, the pellicle of cellulose formed on top of the culture was removed. It was boiled in 1 N NaOH for 20 min, followed by overnight immersion in 0.5 N NaOH to remove cells. Next, it was thoroughly rinsed with distilled water to remove sodium hydroxide and any leftover media. The pellicles were cut into small pieces and homogenized via tissue homogenizer (IKA, T18 Digital) at various rotation speeds to obtain fine slurry of homogenized bacterial cellulose. The concentration of homogenized bacterial cellulose in the slurry was determined by drying a 10-mL sample of the slurry in a hot air oven set at 60 °C for 48 h and weighing the dry solid component that remained. For imaging, homogenized pellicle of bacterial cellulose was lyophilized at −50 °C for 48 h, with pressure kept below 200 mbar in a Christ α12LD

lyophilizer and imaged using MIRA3 TESCAN scanning electron microscope. Gold was sputter coated on the sample before imaging.

Staining of homogenized bacterial cellulose (HBC) using methylene blue

Homogenized bacterial cellulose samples were stained with equal volumes of methylene blue stain at room temperature for 15 min. To remove excess methylene blue, the cellulose was washed using multiple cycles of centrifuge ($3000 \times g$) till the supernatant was free of blue color of the stain.

Fabrication of fiber-reinforced bioplastic

To fabricate agarose bioplastic, two grams agarose powder and 0.4 mL of glycerol were added in 250-mL Erlenmeyer flasks. Deionized water was further added to make the final volume up to 50 mL. The mixture was brought to a boil in a microwave oven set at 800 W for 4 min, which turned the mixture into a viscous solution. The mixture was allowed to cool to around 60 °C and then manually swirled before casting into films. To make the bioplastic films, 20 mL volume of the mixture was poured into 90-mm Petri plates, cooled and dried at 25 °C for 72 h at 50% relative humidity.

Bacterial cellulose reinforced composites were fabricated by adding different volumes of the slurry into the agarose bioplastic to give a final cellulose concentration of 0, 10, 15, 20, 25, 30, 40 and 50% (w/w) with respect to the agarose. Films with stained cellulose fibers were also produced to study the dispersion of fibers in the agarose bioplastic matrix.

Mechanical testing of the composite bioplastics

The thicknesses of the various films were measured using Digimatic micrometer (Mitutoyo Corporation, Japan) and were found to lie between 150 and 400 μm. The thickness of the films increased with the higher amount of cellulose. ASTM D 1708-59 T standard was followed to measure the tensile properties of the samples. The samples were cut into dog-bone-shaped specimens using EpilogLaser CO_2 laser engraving and cutting machine. As per standard, they were incubated at 25 °C and 50% relative humidity for 72 h, and then tested on Instron 3345 tensile testing machine with an initial grip separation of 0.9 inches (22.86 mm) and crosshead speed of 1 mm/min as per the above ASTM standard. Multiple specimens were tested for each sample, and the average ultimate tensile strength was recorded. Zeiss EVO50 scanning electron microscope was used to scan the tensile fractured cross section of neat agarose and composite of agarose and bacterial cellulose. Dispersion quality was assessed on the basis of this analysis.

Effect of reinforcement on swelling properties

Swelling behavior of composite films at three temperatures, 4, 25 and 37 °C, was studied as follows. Water baths containing deionized water for each of the above

temperatures were set. Small strips of bioplastic composites (size 10 mm × 30 mm) were cut and weighed. A strip of the bioplastic film was immersed in each water bath. After every 15 min, the strips were taken out, wiped with filter paper, weighed and then put back into their respective water baths. The measurements were continued for a little over 2 h, by when the successive readings had equalized. The percentage of swelling (S_w), defined by the equation:

$$S_w = \frac{\text{Weight after swelling} - \text{Initial weight}}{\text{Initial weight}} \times 100$$

was plotted as a function of time elapsed.

Thermogravimetric analysis and Fourier transform infrared spectroscopy of fiber-reinforced bioplastic

Thermogravimetric analysis (TGA) was performed on SDT Q600 equipment from TA instruments. The composite films were dried in a vacuum desiccator lined with anhydrous silica gel for 3 days. 10 mg of samples of the composite films was cut, and the TGA was performed in an inert atmosphere of nitrogen gas with a purge rate of 100 mL/min, with temperature rising from ambient conditions to 700 °C at the rate of 10 °C/min. In between, the samples were held at 80 °C for 10 min to remove any absorbed moisture. Fourier transform infrared spectroscopy was done using Bruker Tensor 27. The samples (20 mg) were ground with KBr (100 mg) using mortar and pestle and the spectra were recorded from wavenumber range 400–4000 cm^{-1}.

Degradation studies

Degradation studies were performed under aerobic conditions. Bioplastic composite films were swollen with water and kept in a Petri dish, exposed to ambient conditions in the laboratory. A sheet of biodegradable filter paper (Whatman® No. 1) was used as a positive control; while a sheet of non-biodegradable polyethylene served as a negative control. Both of these were cut to same size as the bioplastic film, and kept moist under similar conditions. All the samples were sterilized before use by soaking in 70% ethanol for 5 min and drying. The films were imaged every week for any changes. At the end of the experiment, the films were removed, dried in a vacuum desiccator for 3 days, and then imaged on a scanning electron microscope (Zeiss EVO50) after gold coating through sputtering.

Results and discussion

Initial observations on bacterial cellulose

Bacterial cellulose harvested from the cultures after 10 days was in the form of pellicles that covered the top surface of culture medium. The pellicles, which were

around 5 mm in thickness, had large quantities of the culture medium absorbed in them. After washing with NaOH and water, bacterial cellulose revealed its characteristic dull white color (Fig. 1a). Scanning electron microscopy of the samples displayed presence of high aspect ratio bacterial cellulose fibers (Fig. 1b).

Upon homogenization with a tissue homogenizer, the bacterial cellulose pellicles turned into a thick white slurry. Scanning electron microscope revealed very high aspect ratio of bacterial cellulose fibers (Fig. 2). The individual fibers were closely stuck together in the form of a mat, indicating that the interfacial adhesion between the fibers was large. This could be due to the presence of large numbers of hydroxyl groups in cellulose structure, which leads to strong hydrogen bonding between the fibers, in addition to the van der Waals interactions between them.

Fig. 1 Initial observations on bacterial cellulose. **a** A pellicle of bacterial cellulose obtained after culturing the *Acetobacter xylinum* bacteria for 10 days in 100-mm Petri dish. The pellicle was in the form of a hydrogel on the top surface of the culture medium. **b** Scanning electron micrograph of a lyophilised sample of the pellicle obtained in **a** exhibits the nano-dimensional cellulose fibers. The diameter of the fibers is less than 100 nm
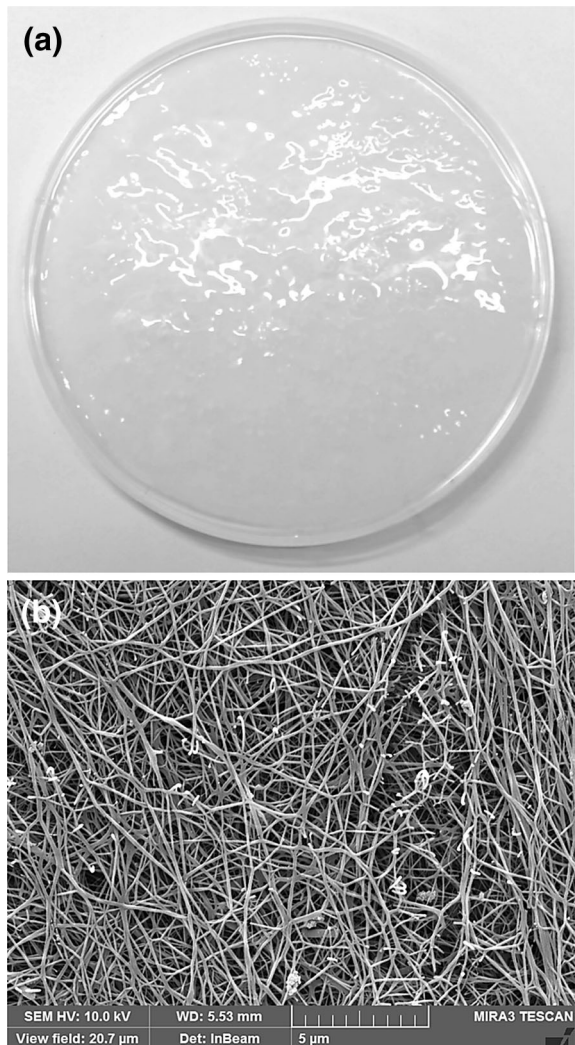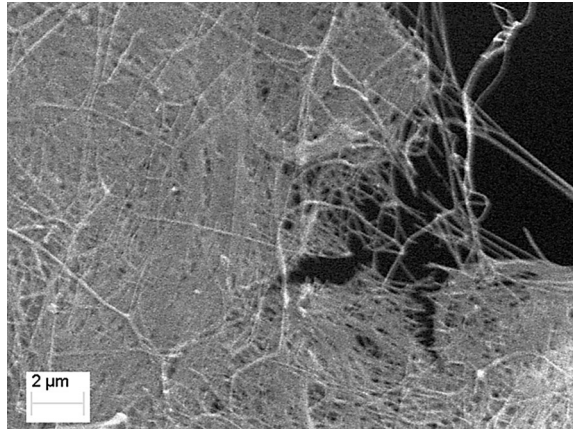
Fig. 2 Scanning electron micrograph of a dried sample of homogenized bacterial cellulose. This reveals that the homogenized fibers have high aspect ratios and they strongly adhere to each other

Changes in ultimate tensile strength as a function of amount of reinforcement

The tensile strength of agarose bioplastic (25.1 MPa) increased with adding bacterial cellulose to a maximum at 60.2 MPa for 20% cellulose before decreasing again (Fig. 3a). The increase in strength of the bioplastic composite was substantial, around 140% compared to that of pure bioplastic. This is because the reinforcing fibers are the main source of strength in a fiber-reinforced composite. The function of the matrix is mostly to hold the fibers together and distribute stresses among individual fibers. Bacterial cellulose fibers possess high degree of crystallinity [38–40], excellent tensile strength of 2 GPa [41–43], and Young's modulus of around 100 GPa [40, 44]. The large number of hydroxyl groups present both in cellulose fibers and the agarose bioplastic matrix could have led to high interfacial interaction between the matrix (bioplastic) and the reinforcement (bacterial cellulose) through hydrogen bonding and van der Waals interactions, permitting efficient distribution of stresses.

We believe that the observed decrease in the strength in case of the composites with very large concentrations of cellulose occurred because the matrix could not hold large amount of reinforcing fibers together. There was not enough matrix to distribute the stresses of applied load to all reinforcing fibers. Since fibers did not have any bonding between them, they slipped due to applied stresses and the strength of the composite decreased. Another possible reason could be agglomeration, and hence resulting in poor transfer of stresses. The optimum concentration of bacterial cellulose for maximum strength was found to be 20% (w/w with respect to agarose). This concentration of bacterial cellulose was chosen for swelling and thermogravimetric tests. Effect of bacterial cellulose concentrations on the elongation properties is shown in Fig. 3b.

The cross section of tensile fractured samples of agarose bioplastic with and without cellulose was imaged using scanning electron microscope. While agarose bioplastic showed relative smooth surface, lot of roughness was observed in agarose–cellulose composite (Fig. 4a, b). The reinforcement and the matrix shared
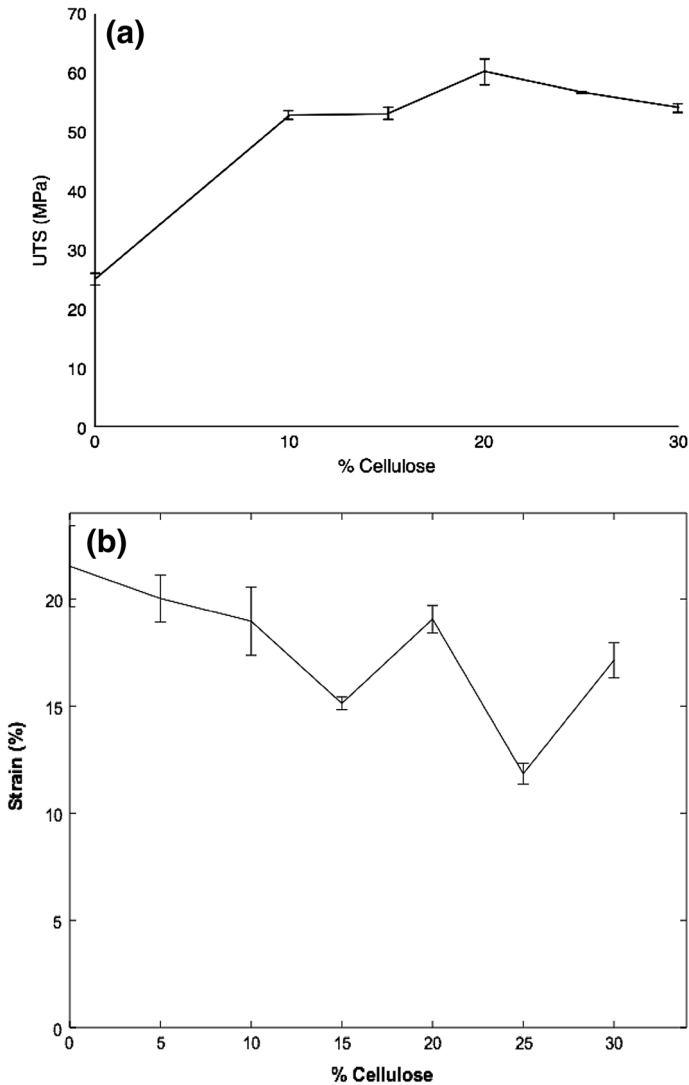
Fig. 3 Tensile testing results. **a** Variation in the strength of composites as a function of amount of bacterial cellulose reinforcement. **b** Variation in the failure strain of composites as a function of amount of bacterial cellulose reinforcement

hydrogen bonds and van der Waal interactions, which is expected to offer better stress transfer from matrix to fiber compared to no interaction between the two. It will be interesting to study the properties of covalently linked cellulose and agarose. Another observation was that the cellulose fibers were uniformly distributed in the film.

Fig. 4 Field emission scanning electron micrograph of tensile fractured cross section of **a** neat agarose and **b** agarose reinforced with 20% homogenized bacterial cellulose. From these images, it is clear that bacterial cellulose is very well dispersed inside the matrix
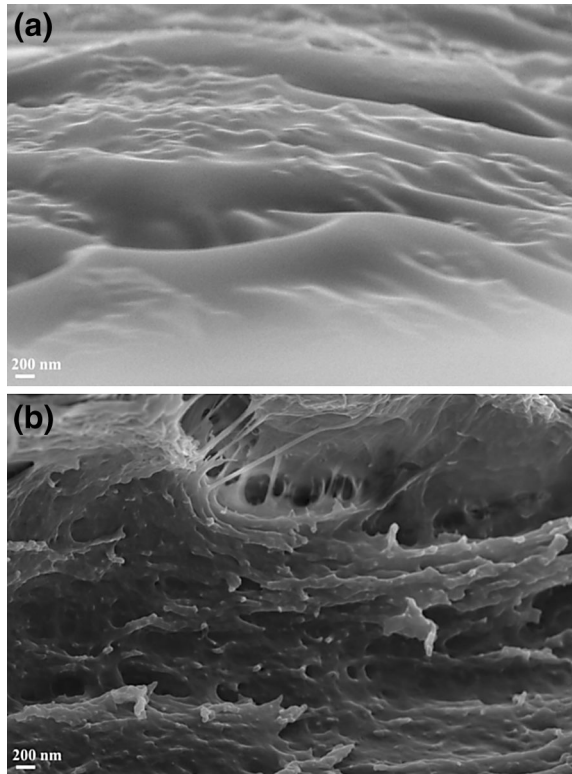
Effect of reinforcement on swelling properties

Agarose bioplastic absorbs large quantities of water, in excess of 700% of its weight at 37 °C [19, 45]. Addition of cellulose to the bioplastic led to a marked reduction in the amount of water absorbed (Fig. 5). For bioplastic composite films with 20% cellulose (w/w with respect to agarose), the amount of water absorbed at 37 °C was around 450% of the weight of the film. Similar trend was also observed at 4 and 25 °C where reinforced bioplastic swelled to a lesser extent than the virgin bioplastic. The rate of swelling of the composite was highest in the beginning for all three test temperatures, and then gradually decreased with time, as the composite films became saturated. The saturation was complete in 120 min. The amount of water absorbed by the composite films increased from 350% at 4 °C to 450% at 37 °C. The reason for the increase in water absorption with increase in temperature lay in the fact that at higher temperatures, the agarose chains within the matrix had more energy, and thus higher mobility. They were able to move apart with ease, generating more space that was taken up by water molecules. It is also worth mentioning that significant swelling occurred within 15 min. The large amount and fast rate of swelling indicated that the chains were relatively unhindered in their movement.
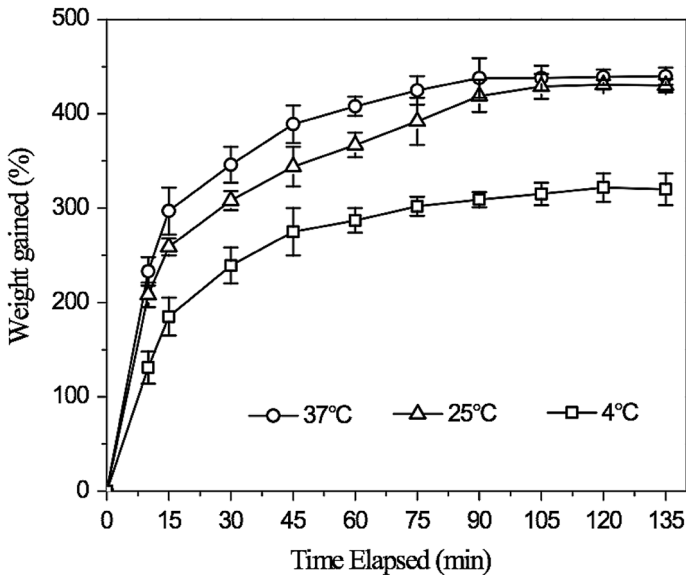
Fig. 5 Swelling curves of composites with 20% bacterial cellulose at 4, 25 and 37 °C as a function of time. The amount of water absorbed increases with temperature and time till a plateau is reached in around 120 min

With the addition of cellulose, the total amount of water absorbed decreased significantly. This could be because the amount of water absorbed is an additive property of the properties of the matrix and the reinforcement, adjusted by appropriate volume fractions. When agarose bioplastic was soaked in water, it swelled, generating a large void fraction. In this way, space was generated which was taken up by water molecules. When bacterial cellulose fibers were added to create a composite, two distinct phases were formed: the matrix and the reinforcement. In the case of agarose–cellulose composites, the agarose matrix could absorb larger quantities of water than the cellulose reinforcement. Although the pellicle of bacterial cellulose was a hydrogel, a porous structure that could accommodate large quantities of water, the individual cellulose fibers are thread-like and devoid of porosity to accommodate water molecules. Thus, the reduction in water retention characteristics in the case of agarose–cellulose composite was largely due to the replacement of part of absorbent matrix by non-absorbing reinforcement phase.

Thermogravimetric analysis and Fourier transform infrared spectroscopy of fiber-reinforced bioplastic

The result of the thermogravimetric test is shown in Fig. 6a. The sharp decrease at 80 °C was due to the loss of absorbed water vapor, since the composite films were held at this temperature for 10 min to ensure complete drying. The other sharp decrease in mass from around 225 to 375 °C occurred due to a variety of physical
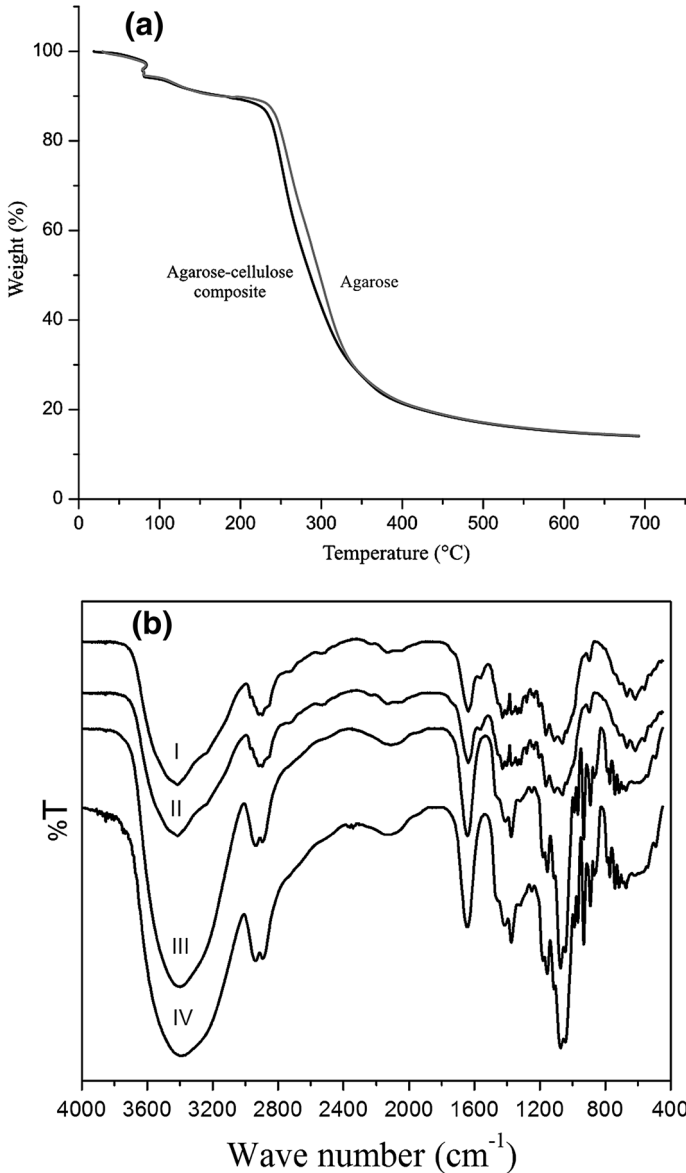
Fig. 6 **a** Thermograms of bioplastic and reinforced composite. The sample of reinforced composite had 20% bacterial cellulose as reinforcement phase. Similarity in the thermograms suggests similar thermal properties in the absence of major chemical changes. **b** Fourier transform infrared spectra of (I) bacterial cellulose, (II) homogenized bacterial cellulose, (III) neat agarose and (IV) agarose/20% homogenized bacterial cellulose

and chemical changes, including loss of glycerol (boiling point of 290 °C) and charring of the composite. The curves became flat towards the right end of the figure, when char and ash, which are stable components, were left behind.

Fig. 7 Degradation studies. Polyethylene sheet (**a**, **d**), bioplastic film (**b**, **e**) and filter paper (**c**, **f**) were ▶
kept under moist conditions. The images show the appearance of composite films on day 0 (**a–c**) and after
3 weeks (**d–f**). While there was no discernible microbial growth on polyethylene sheet, the bioplastic film
and filter paper showed the presence of *dark* colonies of molds. Scanning electron microscopy of the
microbial colonies revealed the existence of fungal hyphae (**g**), confirming the presence of molds. The
diameter of Petri dishes (**a–f**) is 90 mm

There was no major discernible difference between the TGA curves of non-reinforced agarose bioplastic and the reinforced composite, which was because of two reasons. First, the addition of cellulose reinforcements did not produce any chemical changes in agarose chains that could have affected their thermal stability because no visible changes took place in the solution. Second, the chemical composition of cellulose chains is very similar to that of agarose chains; while agarose chains consist of modified galactose residues, cellulose chains consist of glucose residues. Thus, the composite was chemically very similar to the non-reinforced bioplastic matrix. Similar results have also been reported in the literature for starch–cellulose [46] and PVA–cellulose [47] composites.

Identical FTIR spectra of bacterial cellulose and homogenized bacterial cellulose can be observed in Fig. 6b. This is obvious since we performed mechanical treatment of bacterial cellulose that did not lead to any chemical changes in the structure of cellulose. Comparing the FTIR spectra of neat agarose film and agarose/20% homogenized bacterial cellulose film, we can conclude that there is no chemical bond formation between agarose and bacterial cellulose. Broadening of the –OH group can be observed in case of agarose and bacterial cellulose composite as compared to neat agarose film. This property attributes to the physical interaction between –OH group of agarose and bacterial cellulose via hydrogen bonding, which enhances the mechanical properties of the composite by strengthening the interaction and improving the stress transfer between the matrix and used fillers [48–51].

Degradability studies

We selected aerobic microbial degradation as a proxy for the assessment of degradability of the bioplastic. The microorganisms in this case are saprotrophic organisms, which employ chemo-heterotrophic extracellular digestion. The specimens were observed for several weeks for any microbial growth or other changes. While there were no discernible changes observed in the non-biodegradable polyethylene film (Fig. 7a, d), the biodegradable filter paper and bioplastic composite films had perceptible changes (Fig. 7b, c, e, f). There was a heavy growth of microbes on the bioplastic film after 3 weeks. At many places where there was a dense proliferation of microbes, the film had a visually dented appearance with holes, which were a telltale sign of the degenerating film. Similar changes were also observed for the filter paper, though on a more modest scale.

The microbial colonies observed in the case of bioplastic composite films and filter papers had dark patches with mushy and capillaceous appearance, suggestive of fungal growth. Scanning electron micrographs revealed the presence of hyphae,
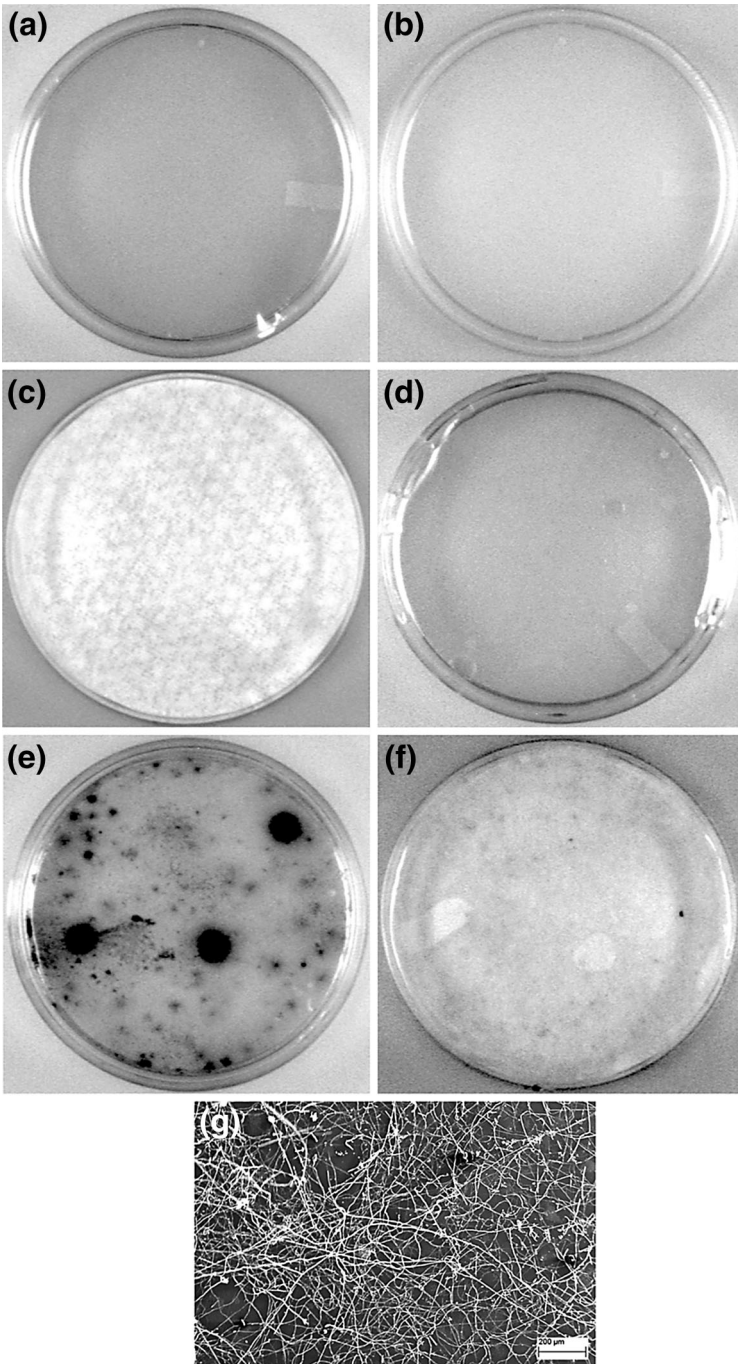
confirming the presence of molds (Fig. 7g). Overall, the study validated the biodegradability of the agarose bioplastic composite films. The biodegradability of agarose bioplastic was even more so than filter paper, which was used as a positive control in the experiments. We believe that the reason lies in the composition and structure of the agarose bioplastic. The bioplastic film consists of carbohydrates and glycerol in a mixture, both of which are rich sources of energy for fungi. Agarose and glycerol are smaller and simpler molecules when compared to long chains of cellulose in paper, and are easier to digest than cellulose. The abundance of food permits the mold population to boom easily.

Conclusions

This study was aimed at synthesis and characterization of agarose films reinforced with bacterial cellulose fibers. It was found that the bacterial cellulose reinforcement enhanced the mechanical and thermal properties of agarose without affecting its biodegradability. Strength of composite bioplastic increased up to a maximum of 60.2 MPa, an increase of 140% compared to virgin bioplastic (tensile strength 25.1 MPa), with the addition of 20% w/w bacterial cellulose. SEM analysis of cross section of fractured samples proved that bacterial cellulose fibers were well dispersed throughout the matrix. There was a marked change in the swelling characteristics of the bioplastic; the amount of water absorbed at 37 °C by the composite was only 62.5% of the amount absorbed by the non-reinforced control sample. It was also observed that there was no significant difference in the thermal properties of the reinforced composite vis-à-vis a non-reinforced control sample. The bioplastic was found to be biodegradable, and thus would not pose serious strain on waste disposal. Hence, reinforcement with cellulose will enlarge the scope of application of the bioplastic, while retaining its most significant attributes.

Compliance with ethical standards

Conflict of interest The authors declare competing financial interest. AA and VV have filed for an Indian patent with Application Number 906/DEL/2015 dated March 31, 2015 and an international patent with Application Number PCT/IB2015/053216 on May 02, 2015. The work demonstrated here is part of the patent.

References

1. Zhang Y, Yuan X, Thompson MR, Liu Q (2012) Characterization of extruded film based on thermoplastic potato flour. J Appl Polym Sci 125:3250–3258
2. Mohanty AK, Tummala P, Liu W, Misra M, Mulukutla PV, Drzal LT (2005) Injection molded biocomposites from soy protein based bioplastic and short industrial hemp fiber. J Polym Environ 13:279–285
3. Gonzalez-Gutierrez J, Partal P, Garcia-Morales M, Gallegos C (2010) Development of highly-transparent protein/starch-based bioplastics. Bioresour Technol 101:2007–2013
4. Vadori R, Mohanty AK, Misra M (2013) The effect of mold temperature on the performance of injection molded poly (lactic acid)-based bioplastic. Macromol Mater Eng 298:981–990
5. Kumaravel S, Hema R, Lakshmi R (2010) Production of polyhydroxybutyrate (bioplastic) and its biodegradation by *Pseudomonas lemoignei* and *Aspergillus niger*. J Chem 7:S536–S542
6. Zarrinbakhsh N, Misra M, Mohanty AK (2011) Biodegradable green composites from distiller's dried grains with solubles (DDGS) and a polyhydroxy (butyrate-*co*-valerate)(PHBV)-based bioplastic. Macromol Mater Eng 296:1035–1045
7. Singh S, Mohanty AK (2007) Wood fiber reinforced bacterial bioplastic composites: fabrication and performance evaluation. Compos Sci Technol 67:1753–1763
8. Reddy N, Yang Y (2010) Citric acid cross-linking of starch films. Food Chem 118:702–711
9. Hutmacher D, Goh J, Teoh S (2001) An introduction to biodegradable materials for tissue engineering applications. Ann Acad Med Singap 30:183–191
10. Şentürk SB, Kahraman D, Alkan C, Gökçe İ (2011) Biodegradable PEG/cellulose, PEG/agarose and PEG/chitosan blends as shape stabilized phase change materials for latent heat energy storage. Carbohydr Polym 84:141–144
11. Tabata M, Shimoda T, Sugihara K, Ogomi D, Serizawa T, Akashi M (2003) Osteoconductive and hemostatic properties of apatite formed on/in agarose gel as a bone-grafting material. J Biomed Mater Res B Appl Biomater 67:680–688
12. Dias AB, Müller CMO, Larotonda FDS, Laurindo JB (2010) Biodegradable films based on rice starch and rice flour. J Cereal Sci 51:213–219
13. Funke U, Bergthaller W, Lindhauer MG (1998) Processing and characterization of biodegradable products based on starch. Polym Degrad Stab 59:293–296
14. Bao X, Hayashi K, Li Y, Teramoto A, Abe K (2010) Novel agarose and agar fibers: fabrication and characterization. Mater Lett 64:2435–2437
15. Sánchez-Salcedo S, Nieto A, Vallet-Regí M (2008) Hydroxyapatite/β-tricalcium phosphate/agarose macroporous scaffolds for bone tissue engineering. Chem Eng J 137:62–71
16. Lewitus DY, Smith KL, Landers J, Neimark AV, Kohn J (2014) Bioactive agarose carbon-nanotube composites are capable of manipulating brain–implant interface. J Appl Polym Sci 131:40297–40304
17. Li X, Gao H, Scrivens WA, Fei D, Thakur V, Sutton MA, Reynolds AP, Myrick ML (2005) Structural and mechanical characterization of nanoclay-reinforced agarose nanocomposites. Nanotechnology 16:2020
18. Le Goff KJ, Gaillard C, Helbert W, Garnier C, Aubry T (2015) Rheological study of reinforcement of agarose hydrogels by cellulose nanowhiskers. Carbohydr Polym 116:117–123
19. Awadhiya A, Kumar D, Verma V (2016) Crosslinking of agarose bioplastic using citric acid. Carbohydr Polym 151:60–67
20. Yang CX, Gao C, Wan YZ, Tang TT, Zhang SH, Dai KR (2011) Preparation and characterization of three-dimensional nanostructured macroporous bacterial cellulose/agarose scaffold for tissue engineering. J Porous Mater 18:545–552
21. Fernandez-Cossio S, Leon-Mateos A, Sampedro FG, Oreja MT (2007) Biocompatibility of agarose gel as a dermal filler: histologic evaluation of subcutaneous implants. Plast Reconstr Surg 120:1161–1169
22. Kao JM, Rose R, Yousef M, Hunter SK, Rodgers VG (1999) In vivo biocompatibility evaluation of Cibacron blue-agarose. J Biomed Mater Res 47:537–542
23. Shankar S, Rhim J-W (2016) Preparation of nanocellulose from micro-crystalline cellulose: the effect on the performance and properties of agar-based composite films. Carbohydr Polym 135:18–26
24. Rhim J-W, Reddy JP, Luo X (2015) Isolation of cellulose nanocrystals from onion skin and their utilization for the preparation of agar-based bio-nanocomposites films. Cellulose 22:407–420

25. Leitner J, Hinterstoisser B, Wastyn M, Keckes J, Gindl W (2007) Sugar beet cellulose nanofibril-reinforced composites. Cellulose 14:419–425

26. Oishi Y, Nakaya M, Matsui E, Hotta A (2015) Structural and mechanical properties of cellulose composites made of isolated cellulose nanofibers and poly (vinyl alcohol). Compos A Appl Sci Manuf 73:72–79

27. Sonker AK, Tiwari N, Nagarale RK, Verma V (2016) Synergistic effect of cellulose nanowhiskers reinforcement and dicarboxylic acids crosslinking towards polyvinyl alcohol properties. J Polym Sci Part A Polym Chem 54:2515–2525

28. Favier V, Canova GR, Cavaillé JY, Chanzy H, Dufresne A, Gauthier C (1995) Nanocomposite materials from latex and cellulose whiskers. Polym Adv Technol 6:351–355

29. Gabr MH, Elrahman MA, Okubo K, Fujii T (2010) A study on mechanical properties of bacterial cellulose/epoxy reinforced by plain woven carbon fiber modified with liquid rubber. Compos A Appl Sci Manuf 41:1263–1271

30. Li M-C, Wu Q, Song K, Lee S, Qing Y, Wu Y (2015) Cellulose nanoparticles: structure–morphology–rheology relationships. ACS Sustain Chem Eng 3:821–832

31. Deng F, Ge X, Zhang Y, Li MC, Cho UR (2015) Synthesis and characterization of microcrystalline cellulose-graft-poly (methyl methacrylate) copolymers and their application as rubber reinforcements. J Appl Polym Sci 132:42666–42675

32. Favi PM, Ospina SP, Kachole M, Gao M, Atehortua L, Webster TJ (2016) Preparation and characterization of biodegradable nano hydroxyapatite–bacterial cellulose composites with well-defined honeycomb pore arrays for bone tissue engineering applications. Cellulose 23:1263–1282

33. Kirdponpattara S, Khamkeaw A, Sanchavanakit N, Pavasant P, Phisalaphong M (2015) Structural modification and characterization of bacterial cellulose–alginate composite scaffolds for tissue engineering. Carbohydr Polym 132:146–155

34. Chang W-S, Chen H-H (2016) Physical properties of bacterial cellulose composites for wound dressings. Food Hydrocolloids 53:75–83

35. Yin N, Stilwell MD, Santos TM, Wang H, Weibel DB (2015) Agarose particle-templated porous bacterial cellulose and its application in cartilage growth in vitro. Acta Biomater 12:129–138

36. El-Saied H, El-Diwany AI, Basta AH, Atwa NA, El-Ghwas DE (2008) Production and characterization of economical bacterial cellulose. Bioresources 3:1196–1217

37. Hestrin S, Schramm M (1954) Synthesis of cellulose by *Acetobacter xylinum*. 2. Preparation of freeze-dried cells capable of polymerizing glucose to cellulose. Biochem J 58:345

38. Ohad I, Danon D, Hestrin S (1962) Synthesis of cellulose by *Acetobacter xylinum* V. Ultrastructure of polymer. J Cell Biol 12:31–46

39. Brown RM, Willison JH, Richardson CL (1976) Cellulose biosynthesis in *Acetobacter xylinum*: visualization of the site of synthesis and direct measurement of the in vivo process. Proc Natl Acad Sci 73:4565–4569

40. Guhados G, Wan W, Hutter JL (2005) Measurement of the elastic modulus of single bacterial cellulose fibers using atomic force microscopy. Langmuir 21:6642–6646

41. Wan YZ, Hong L, Jia SR, Huang Y, Zhu Y, Wang YL, Jiang HJ (2006) Synthesis and characterization of hydroxyapatite–bacterial cellulose nanocomposites. Compos Sci Technol 66:1825–1832

42. Yano H, Sugiyama J, Nakagaito AN, Nogi M, Matsuura T, Hikita M, Handa K (2005) Optically transparent composites reinforced with networks of bacterial nanofibers. Adv Mater 17:153–155

43. Gardner DJ, Oporto GS, Mills R, Samir MASA (2008) Adhesion and surface issues in cellulose and nanocellulose. J Adhes Sci Technol 22:545–567

44. Hsieh YC, Yano H, Nogi M, Eichhorn SJ (2008) An estimation of the Young's modulus of bacterial cellulose filaments. Cellulose 15:507–513

45. Awadhiya A, Tyeb S, Rathore K, Verma V (2016) Agarose bioplastic based drug delivery system for surgical and wound dressings. Eng Life Sci. doi:10.1002/elsc.201500116

46. Srithongkham S, Vivitchanont L, Krongtaew C (2012) Starch/cellulose biocomposites prepared by high-shear homogenization/compression molding. J Mater Sci Eng B 2:213–222

47. Lee S-Y, Mohan D, Kang I-A, Doh G-H, Lee S, Han S (2009) Nanocellulose reinforced PVA composite films: effects of acid treatment and filler loading. Fibers Polym 10:77–82

48. Roohani M, Habibi Y, Belgacem NM, Ebrahim G, Karimi AN, Dufresne A (2008) Cellulose whiskers reinforced polyvinyl alcohol copolymers nanocomposites. Eur Polym J 44:2489–2498

49. Phua SL, Yang L, Toh CL, Huang S, Tsakadze Z, Lau SK, Mai Y-W, Lu X (2012) Reinforcement of polyether polyurethane with dopamine-modified clay: the role of interfacial hydrogen bonding. ACS Appl Mater Interfaces 4:4571–4578

50. Zhang W, Dehghani-Sanij AA, Blackburn RS (2008) IR study on hydrogen bonding in epoxy resin–silica nanocomposites. Prog Nat Sci 18:801–805
51. Aztatzi-Pluma D, Castrejón-González EO, Almendarez-Camarillo A, Alvarado JF, Duran-Morales Y (2016) Study of the molecular interactions between functionalized carbon nanotubes and chitosan. J Phys Chem C 120:2371–2378